Automatic lung segmentation method in computed tomography scans

Automatic lung segmentation method in computed tomography scans

F Shariaty[1, 2], S Hosseinlou[1] and V Yu Rud' [2,3]

[1] Department of Electrical Engineering, University of Qom, Qom, Iran
[2] Peter the Great St. Petersburg Polytechnic University, St. Petersburg 195251, Russia
[3] All-Russian Research Institute of Phytopathology, Moscow Region 143050, Russia

E-mail: Shariaty3@gmail.com

Abstract. Lung segmentation in Computed Tomography (CT) images is one of the important steps in Computer Aided Diagnosis (CADx) systems. This paper has proposed a completely automatic algorithm for recognition and segmentation of lungs in 3D pulmonary X-ray CT images. The advantage of this method is separation of attached nodules to the lung wall which are removed in ordinary lung segmentation methods. This method is based on thresholding algorithm that identifies attached nodules with some morphological operations. This method applied to 20 lung CT images has shown that eventually the lungs were correctly segmented. The advantage of using a simple thresholding algorithm is high speed, e.g. the time of the lung segmentation for 300 images is less than 10 seconds.

1. Introduction

Lung cancer is the leading reason of cancer related mortality in the world. Being 80 % to 85 % of lung cancers, non-small cell lung carcinoma (NSCLC) is the most common epithelial lung cancerous nodules [1]. The primary treatment of NSCLCs is radical surgery resection, followed by increasingly using pre- and post-operative chemical therapy. Recent advances in understanding of molecular genetics and pathology of NSCLS leads to increasing using of molecular therapy [2] and immunotherapy [3]. Survival is directly related to the stage of lung cancer at the time of diagnosis. If lung cancer is detected at its earliest stage, the five-year survival rate can reach 70 % and otherwise the average five-year survival rate after lung cancer diagnosis is about 15 % [4-6]. Even though the diagnosis of the small nodules in CT scan is always challenging in the radiology, the proficiency of the computer-aided diagnosis (CADx) systems in early detection of them is well investigated in the recent literature [7-9]. The CAD systems for lung nodule detection work in four steps [10-12]:

1. **Image pre-processing**: in lung CT scans, pre-processing techniques increases the visibility and sharpness of pulmonary nodules;
2. **Lung segmentation**: It is essential to extract lungs from muscles, fats etc. This step by improving accuracy and precision, plays a vital role in CAD systems function;
3. **Candidate nodule detection**: A pulmonary nodule is almost spherical shaped with size range 4 to 30 millimeter;
4. **Nodule classification**: After the candidate nodules are detected the resultant set of nodules must be classified into two nodules and non-nodules groups.

Since the lung is a complex organ and includes various structures such as vessels, gaps, bronchus or pleura, which can be close to the lung nodule, lung extraction is one of the most important steps in

CAD systems. This step helps to speed up operations in the system, as well as increasing the accuracy of nodule diagnosis and nodule segmentation. The importance of lung segmentation is due to presence of different nodule types. Nodules are classified into two categories in terms of their location in lungs[13]: non-attached nodules (well-circumscribed nodules) and attached nodules (juxta-pleural, vascularized and pleural-tail), as shown in figure 1. Segmentation of non-attached nodules is usually performed with high accuracy but in order to segment entire attached nodules, lungs must extract from the surrounding area.

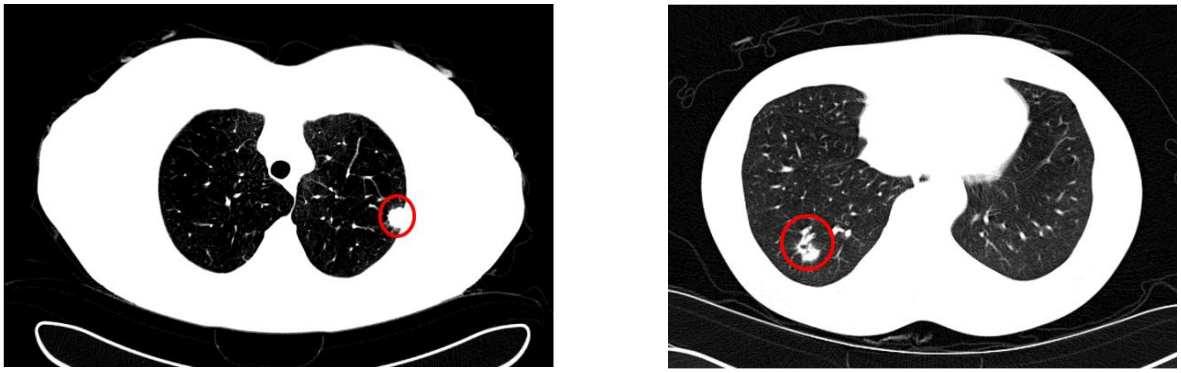

(a) (b)

Figure 1. Categorization lung nodules in terms of their location: (a) attached nodule, (b) non-attached nodule.

Many methods [14-17] have been proposed to segment the lung automatically in volumetric CT images. J.pu et al. [18] proposed a lung segmentation algorithm called adaptive border marching (ABM). This method detects the lung border with a geometric method while the lung includes juxta-pleural nodules. The segmentation time of a typical case is 1 min which is higher than proposed method that presented in this paper. H. Chung et al. [19] proposed a model based on Chane-Vese active contour to segment lung with juxta-pleural nodule. One of the most common techniques for lung images segmenting is thresholding approach [17, 20], wherein the natural contrast between the low-density lungs and the surrounding high-density chest wall is used for lung segmentation. For instance the authors in [20] proposed a method based on 3 steps: (1) image preprocessing to remove background, (2) computation a threshold to identify lung tissue, and (3) refinement of the initial segmented regions to prune incorrectly detected airways and separate fused right and left lungs.

2. Materials and Methods

The lung CT images of the LIDC-IDRI database [21] are employed in the experiments. The Lung Image Database Consortium (LIDC) and Image Database Resource Initiative (IDRI) completed such a database, establishing a publicly available reference for the medical imaging research community. It is an international resource for development, training, and analysing of CADx methods for lung cancer detection and diagnosis. In this study, we used a dataset of 10 CT scans that have juxta-pleural nodules. The number of slices per CT scan ranged from 126 to 352 and therefore the total number of slices was 2864. Every slice includes a size of 512 × 512 pixels with a 12-bit gray scale resolution in Hounsfield Units (HU).

The proposed method includes the following major processing steps: First the lung lesion segmented from surrounding area using optimal thresholding method and make a 3D mask. Then each mask slice compared with the previous slice in order to find nodules attached to the lung wall. In presence of juxta-pleural nodules a reconstruction algorithm consists of several morphological operations has been applied to rectify the mask image.

2.1. Thresholding

In the CT image data, air will seem with a mean intensity of roughly 1000 Hounsfield units (HU), most lung tissue will be within the range of 500 HU to 910 HU, whereas the chest wall, blood, and bone will be rather more dense (well higher than 500 HU) [16]. So, for separate the voxels corresponding to the lung tissue from voxels corresponding to the surrounding anatomy, a fixed threshold can be used. Rather than using a fixed threshold, we substitute optimal thresholding [17, 22] to automatically select a segmentation threshold. Optimal thresholding is an automated thresholding method that optimizes the threshold value to fit the image. In this step, the image is assumed to consist two types of voxels: 1) the lung voxels which have higher Hounsfield values and 2) the non-lung voxels which have lower Hounsfield values. The optimal threshold is selected through an iterative procedure. *T*i is assumed the threshold amount at step i. *T*i is applied to the input image to separate lung- from non-lung voxels. Let μ_a and μ_b be the mean gray level of the lung voxels and non-lung voxels after segmentation with threshold *T*i. Then the new threshold amount for next step calculates with Eq.1.

$$T_i = \frac{\mu_a + \mu_b}{2} \tag{1}$$

This iterative updating is repeated until there is no change in the threshold (*T*i = *T*i + 1). The initial Hounsfield threshold is *T*0 = - 1000. With applying this threshold, the initial mask is generated that illustrated in figure 2(B). After fill the holes in this image and select the largest area, figure 2(C) is reached. After inversing figure 2(B) and applying logical "AND" between it and figure 2(C), figure 2(D) is obtained. Then with applying morphological hole filling in figure 2(D), figure 2(E) is obtained which is the final mask of this step.

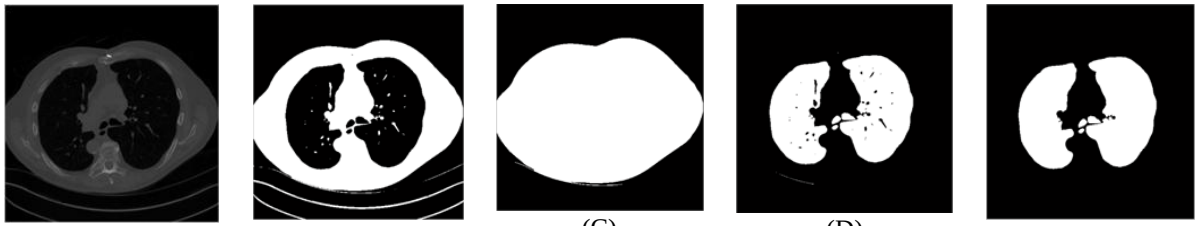

(A) (B) (C) (D) (E)

Figure 2. The steps of thresholding algorithm to reach the lung mask: A) Input Image; B) Segmentation with optimal threshold; C) Fill the holes and select largest area; D) Logical "AND" between C and inverse B; E) Fill the holes.

Until here we arrived a lung mask but this mask has a problem when the lung has juxta-pleural nodule that illustrates in figure 3. If the juxta-pleural nodule exists in lung, the reconstruction algorithm is applied in order to detect and solve errors.

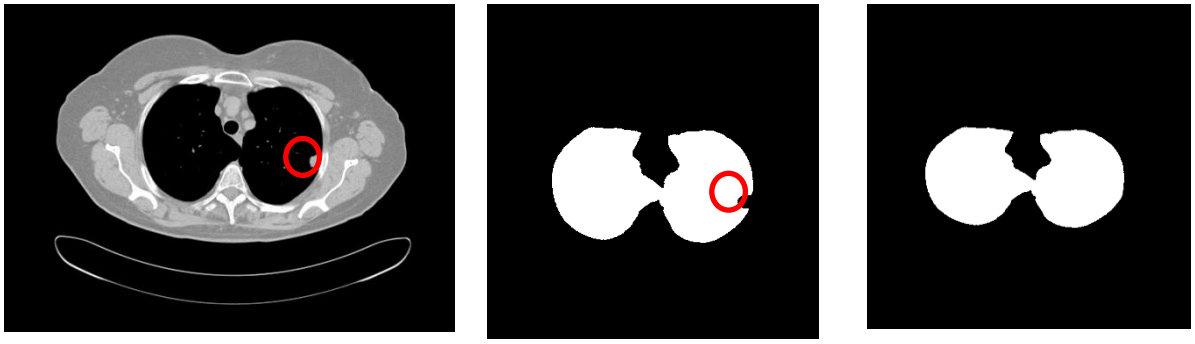

(A) (B) (C)

Figure 3. Segmentation of the lung with juxta-pleural nodule: (A) input image; (B) segmented image with error; (C) segmented image after reconstruction operation.

2.2. Reconstruction

The reconstruction operation is based on comparing each slice with the previous slice. For this comparison, difference of each slice with the previous slice calculated according to Eq.2.

$$Difference = Slice_{i-1} - slice_i \tag{2}$$

This step is illustrated in figure 4 for the lung with attached nodule (figure 4(B)) and without it (figure 4(A)). In the next step the narrower lines from 4 pixels and smaller areas from 10 pixels are eliminated by morphological operations. This step removes the areas that are visible in figure 4 and then only attached nodule stay in image. However, in some images, these two limitations of area and thickness are not enough to detect attached nodules so other conditions should apply. The first condition that applies to white areas is the area limit that should not exceed 300 pixels because usually the attached nodules to the lung wall are not in this range. In the next step, the circularity of the areas is investigated. This value is calculated by Eq.3 that should be bigger than 0.3.

$$C = \frac{4 \times \pi \times Area}{Perimeter^2} \tag{3}$$

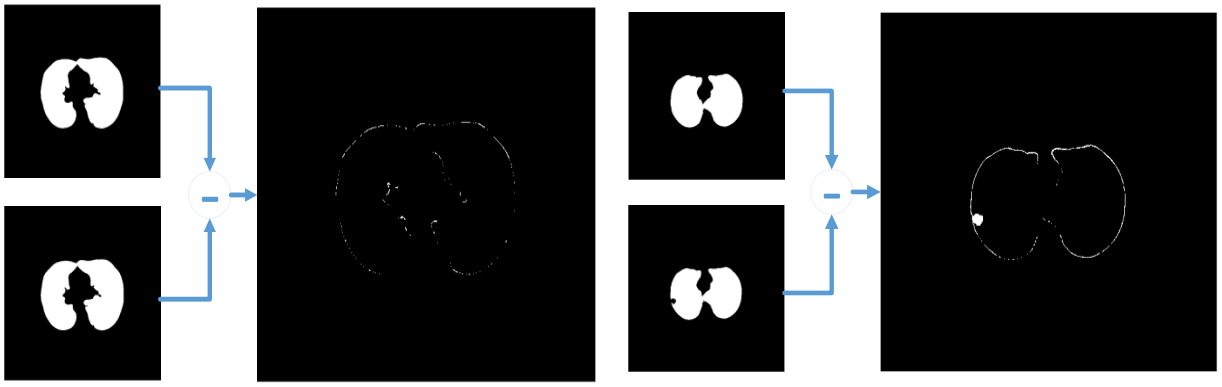

(A) (B)

Figure 4. Difference of each slice with the previous slice: (A) lung without attached nodule; (B) lung with attached nodule.

At the end of this process, only the area of attached nodule remains, which add to the initial lung mask produced at the thresholding stage. In a CT scan with “n” slices that have attached nodules, the

process of calculating the difference must performed "n" time in order to identify and add attached nodule in all of the "n" slices.

3. Results

Two periods of implementation this lung segmentation algorithm are shown in figure 5. In the first row of figure 5, the initial masks for 5 slices of a lung CT image are illustrated that include attached nodule. As shown, 3 slices of this CT images have nodules and need reconstruction algorithm. According to the proposed algorithm, first the difference between each mask slice and next mask slice computed, as shown in second row of figure 5. The attached nodule only visible in the difference

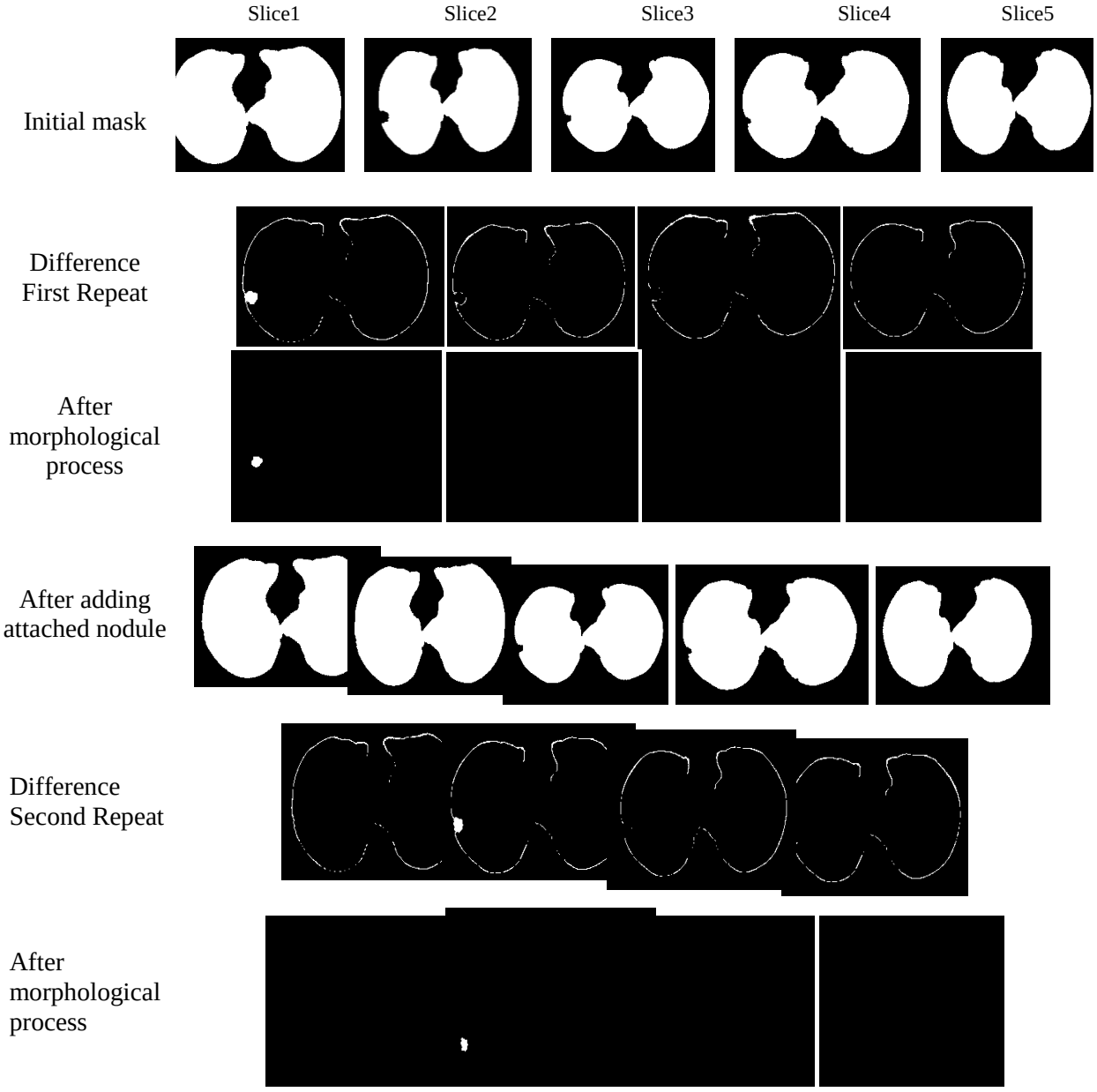

Figure 5. The steps of proposed algorithm.

between the first and second slices, and since the second and third slices are both with attached nodule,

the nodule is not identified in their difference. In the next step, extra white areas are removed and only the attached nodule to the lung wall remains. Finally, in the 4th row of figure 5 this nodule mask added to the initial lung mask and the first period of reconstruction is done. With inception of the next operation period, the difference between all slices with next of them calculated again, as shown in 5th row of figure 5, and the attached nodule to the lung wall in third slice is visible. Then after removal of extra white areas, the nodule added to initial lung mask and the second period of reconstruction is done. The process of adding attached nodule to the initial mask should be repeated in 4th slice, so that in this image which have 3 slices with attached nodule, repetition is required three times to reconstruction initial mask.

Each period of this operation for a lung CT image that has about 300 slices done about 3 seconds. The performing this lung segmentation method takes about 8 to 10 seconds if the reconstruction image is required in three slides. This implementing time is very convenient and short for lung segmentation algorithm, which has been used to speed up works.

This method has been tested on 10 lung CT scans, which totally have 56 slices with attached nodules and in result, this algorithm is very satisfying and suitable for fast applications.

4. Conclusion

We have proposed a new method for segmentation lungs in CT scans based on thresholding algorithm. This method has a reconstruction operation to detect the attached nodules and add them to the lung mask. The results of implementation this algorithm show high speed of it and is more optimal in comparison to other complex algorithms. This segmentation methods could be considered as a potential CADx tool for physicians in the clinical processes. It is desirable to use these methods with the nuclear magnetic resonance method and optical methods, which are more safety for health compared to CT scans [23-33]. This increases the reliability of the diagnosis (lung cancer), especially at the initial stage of disease evolution.

References

[1] Molina J R, Yang P, Cassivi S D, Schild S E and Adjei A A 2008 *In Mayo Clinic Proceedings* **83(5)** 584-594
[2] Barr Kumarakulasinghe N, Zanwijk N V and Soo R A 2015 *Respirology* **20(3)** 370-378
[3] Massarelli E, Papadimitrakopoulou V, Welsh J, Tang C and Tsao A S 2014 *Translational lung cancer research* **3(1)** 53
[4] Nesbitt J C, Putnam Jr J B, Walsh G L, Roth J A and Mountain C F 1995 *Annals of thoracic surgery* **60(2)** 466-472
[5] Humphrey L L, Teutsch S and Johnson M 2004 *Annals of Internal Medicine* **140(9)** 740-753
[6] Flehinger B J, Kimmel M and Melamed M R 1992 *Chest* **101(4)** 1013-1018
[7] Tekade R 2018 *Asian journal for convergence in technology (AJCT)-UGC listed* **34** 342
[8] Mahesh S, Rakesh S and Patil V C 2018 *AIP Conference Proceedings* **1952(1)** 020101
[9] Taher F 2017 *International Conference on Infocom Technologies and Unmanned Systems (Trends and Future Directions) (ICTUS)* 1-1
[10] Bhavanishankar K and Sudhamani M V 2015 *Int. J. Cybern*. **4(1)** 27-40
[11] Likhitkar V K, Gawande U. and Hajari K O 2014 *IOSR J Comput Eng*, **16(1)** 5-11
[12] Alilou M, Kovalev V, Snezhko, E and Taimouri V 2014 *Image Analysis & Stereology* **33(1)** 13
[13] Farag A A, El Munim H E A, Graham J H and Farag A A 2013 *IEEE Transactions on Image Processing* **22(12)** 5202-5213
[14] Bartz D, Mayer D, Fischer J, Ley S, Rio A D, Thust S and Straßer W 2003 *Proceedings of the 14th IEEE Visualization 2003 (VIS'03)* 24
[15] Ukil S and Reinhardt J M 2004 *Medical Imaging: Image Processing* **5370** 1066-1076
[16] Brown M S, Mcnitt-Gray M F, Mankovich N J, Goldin J G, Hiller J, Wilson L S. and Aberie D R 1997 *IEEE transactions on medical imaging* **16(6)** 828-839
[17] Hu S, Hoffman E A and Reinhardt J M 2001 *IEEE transactions on medical imaging* **20(6)** 490

[18] Pu J, Roos J, Chin A Y, Napel S, Rubin G D and Paik D S 2008 *Computerized Medical Imaging and Graphics* **32(6)** 452-462
[19] Chung H, Ko H, Jeon S J, Yoon K H and Lee J 2018 *IEEE journal of translational engineering in health and medicine* **6** 1-13
[20] Leader J K, Zheng B, Rogers R M, Sciurba F C, Perez A, Chapman B E and Gur D 2003 *Academic radiology* **10(11)** 1224-1236
[21] Armato S G, McLennan G, Bidaut L, McNittGray M F, Meyer C R, Reeves A P and Kazerooni E A 2011 *Medical physics* **38(2)** 915-931
[22] Sonka M, Hlavac V and Boyle R 2014 *Cengage Learning*
[23] Nepomnyashchaya E K, Velichko E N and Aksenov E T 2016 *Journal of Physics: Conference Series* **769(4)** 012025
[24] Nepomnyashchaya E K, Akenov E T, Bogomaz T A and Velichko E N 2015 *Journal of Optical Technology (A Translation of Opticheskii Zhurnal)* **82** 162-165
[25] Nepomnyashchaya E K, Cheremiskina A V, Velichko E N, Aksenov E T and Bogomaz E T 2015 *Journal of Physics: Conference Series* **643(1)** 012018
[26] Davydov V V, Cheremiskina A V, Velichko E N and Karseev A Yu 2014 *Journal of Physics: Conference Series* **541(1)** 012006
[27] Davydov V V, Dudkin V I, Velichko E N and Karseev A Yu 2015 *Journal of Optical Technology (A Translation of Opticheckii Zhurnal)* **82(3)** 132-135
[28] Rykin E V, Moroz A V, Smirnov K J, Davydov V V and Yushkova V V 2018 *MATEC Web of Conference* **245** 12002
[29] Davydov V V, Dudkin V I, Myazin N S and Rud' V Yu 2018 *Instruments and Experimental Techniques* **61** 140–147
[30] Davydov V V, Velichko E N, Myazin N S and Rud' V Yu 2018 *Instruments and Experimental Techniques* **61** 116–122
[31] Rud`V Yu, Rud` Yu V, Shpunt V Ch and Terukov E I 2016 *Optical Memory & Neural Networks (Information Optics)* **25** 40
[32] Davydov R V, Antonov V I and Moroz A V 2018 *Proceedings of the 2018 IEEE International Conference on Electrical Engineering and Photonics, EExPolytech 2018* (Saint-Petersburg) 8564378 236-239